Scaling properties of Tan's contact: Embedding pairs and correlation effect in the Tonks-Girardeau limit

F. T. Sant'Ana,[1,2] F. Hébert,[1] V. G. Rousseau,[3] M. Albert,[1] and P. Vignolo[1]
[1]*Institut de Physique de Nice, Université Côte d'Azur, CNRS, Nice, France*
[2]*São Carlos Institute of Physics, University of São Paulo, 13566-590, São Carlos, SP, Brazil*
[3]*5933 Laurel Street, New Orleans, Louisiana 70115, USA*

(Received 23 August 2019; published 4 December 2019)

We study Tan's contact of a one-dimensional quantum gas of N repulsive identical bosons confined in a harmonic trap at finite temperature. This canonical ensemble framework corresponds to the experimental conditions, with the number of particles being fixed for each experimental sequence. We show that in the strongly interacting regime, the contact rescaled by the contact at the Tonks-Girardeau limit is a universal function of two parameters: the rescaled interaction strength and temperature. This means that all pair and correlation effects in Tan's contact are embedded in Tan's contact in the Tonks-Girardeau limit.

DOI: 10.1103/PhysRevA.100.063608

I. INTRODUCTION

Many-body quantum physics is a cornerstone of modern physics and a key to understanding future technologies such as high-T_c superconductivity or quantum computing. However, an accurate description of strongly correlated quantum systems, for an arbitrary number of particles, is often a challenge without a simple solution. Apart from the very specific family of integrable systems [1–11] where all observables can, in principle, be predicted theoretically, our knowledge is, in general, limited to simple situations such as two particles [12–14], solutions that hold in the thermodynamic limit [15,16], low-energy physics [17], or mean-field descriptions for many-body systems [18,19]. It is therefore quite difficult to extract general information such as the scaling of physical observables with respect to the number of particles for generic situations.

For the case of quantum particles with pointlike interactions, short-range correlations are embedded in Tan's contact C_N [20–22]. This quantity, which is proportional to the probability that two particles approach each other infinitely close, determines the asymptotic behavior of the momentum distribution $n(k)$, $C_N = \lim_{k\to\infty} k^4 n(k)$, with k being the momentum divided by $\hbar$. This observable can be measured via time-of-flight techniques [23–25], with radio-frequency spectroscopy [26,27], Bragg spectroscopy [28], by measuring the energy variation as a function of the interaction strength [24], or by looking at three-body losses in quantum mixtures [29]. This central quantity is a function of the interaction energy, density-density correlations function, trapping configuration, temperature, as well as magnetization [30,31], and thus depends in a nontrivial way on the nature and the number N of particles. Therefore, even in one dimension, the behavior of C_N is not completely clarified, especially in trapped systems, despite many theoretical investigations [30,32–35]. For one-dimensional (1D) bosons (and/or fermions) trapped in a harmonic potential of frequency ω, it has been shown that in the thermodynamic limit, at zero temperature, the contact rescaled by $N^{5/2}$ is a universal function of one scaling parameter: $z = a_{ho}/(|a_{1D}|\sqrt{N})$ [15,34]. This holds also at finite temperature, in the grand-canonical ensemble: the contact rescaled by $N^{5/2}$ is a universal function of two scaling parameters, z and $\xi_T = |a_{1D}|/\lambda_{DB}$, or, equivalently, z and $\tau = T/T_F$ [16,36], with a_{1D} being the 1D scattering length, $a_{ho} = \sqrt{\hbar/(m\omega)}$ the harmonic oscillator length, m the mass, $\lambda_{DB} = \sqrt{2\pi\hbar^2/mk_BT}$ the de Broglie thermal wavelength, $T_F = N\hbar\omega/k_B$ the Fermi temperature, and k_B the Boltzmann constant. However, for systems with a small number of particles, the $N^{5/2}$ scaling fails. In the zero-temperature limit [37], it is possible to change the paradigm and to introduce a different scaling form that holds from $N = 2$ to infinity. At finite temperature, in the grand-canonical ensemble, the $N^{5/2}$ scaling holds for $N > 10$ [16]. However, corrections at a small number of particles have, to our knowledge, not yet been studied in 1D and the important question of the relevance of the statistical ensemble has not been addressed. The latter is indeed a crucial point since ultracold-atom experiments are canonical or, more often, an average over canonical ensembles, but not grand canonical, and scaling properties are obviously strongly affected by the statistical distribution of particles numbers. In fact, in ultracold experiments, in each experimental sequence, N atoms are charged in a three-dimensional trap. Then the atoms are separated in several light wires created by the interference of two propagating laser beams [38]. The atomic gas in the wires can be considered as one dimensional if the interaction and thermal energies are lower than the energy scale of the radial confinement $\hbar\omega_\perp$, with $\omega_\perp$ being the radial harmonic oscillator frequency [39]. Otherwise, atoms can be directly trapped in a single 1D tube with a strong radial confinement [40]. In both cases, the relation between the 1D scattering length a_{1D} and the 3D one a_{3D} is given by $a_{1D} = -a_\perp^2/a_{3D}$, where $a_\perp = \sqrt{\hbar/(m\omega_\perp)}$ [41].

 ©2019 American Physical Society

In this paper, we study the canonical Tan's contact for a small number of harmonically trapped Lieb-Liniger bosons.

We show that in the strongly interacting regime, the contact for N bosons at temperature T and with repulsive interaction, divided by the contact for the same number of bosons and temperature but in the regime of infinite repulsions, is an N-independent function of z and τ. Namely, all the nontrivial particle-number dependence is embedded in the contact in the infinite interaction limit, even at finite temperature, which is the main result of this work. The regime of infinite repulsions in one dimension corresponds to the so-called Tonks-Girardeau limit. In this regime, the infinite repulsions, due to the low dimensionality, play the role of a sort of Pauli principle so that bosons "behave" as noninteracting fermions. Another result is that we provide an analytical expression for the N dependence of the canonical contact in the Tonks-Girardeau limit. Our formula is a conjecture that works extremely well over the whole temperature range. The consequence of these two results is that we can explicitly express the canonical contact for N harmonically trapped Lieb-Liniger bosons in the intermediate- and strong-interaction regime ($z > 1$), for any value of N and any temperature T.

The paper is organized as follows. In Sec. II, we introduce the physical system and define the canonical Tan's contact. This observable is then evaluated exactly in two special situations: for two identical bosons at any interaction strength and any temperature and for N identical bosons in the Tonks-Girardeau limit (infinite coupling). In the general situation, namely, for intermediate interaction strength and for $N > 2$, we calculate Tan's contact by means of quantum Monte Carlo (QMC) simulations. The scaling properties of the canonical contact are then analyzed in Sec. III. After reviewing the results previously obtained in the strongly interacting limit at zero temperature [37], we analyze the large-temperature scaling of the contact in the same limit. By comparing these two limits, we propose an explicit form of the contact scaling function holding in the strongly interacting limit and at any temperature, which makes our numerical data overlap for different number of atoms N with only a few-percent discrepancy. In Sec. IV, we compare the canonical contact with the grand-canonical one. At large temperature, the canonical and grand-canonical contacts are both proportional to the two-boson contact. This does not hold at smaller temperatures. Finally, our concluding remarks are given in Sec. V.

II. CANONICAL TAN'S CONTACT

We consider a gas of N identical interacting bosons of mass m trapped in a 1D harmonic confinement. This system is described by the Hamiltonian

$$H = \sum_{i=1}^{N}\left(-\frac{\hbar^2}{2m}\frac{\partial^2}{\partial x_i^2} + \frac{1}{2}m\omega^2 x_i^2\right) + g\sum_{i<j}\delta(x_i - x_j), \quad (1)$$

where the repulsive interaction strength g depends on the 1D scattering length as $g = -2\hbar^2/ma_{1D}$, if $a_\perp \gg a_{3D}$ [41]. At finite temperature T, in the canonical ensemble, the contact for N bosons, $C_N^c(g, T)$, can be deduced from the free energy F by exploiting Tan's sweep relation [20],

$$\begin{aligned} C_N^c(g,T) &= -\frac{m^2}{\pi\hbar^4}\frac{\partial F}{\partial g^{-1}} \\ &= -\frac{m^2}{\pi\hbar^4}\frac{\sum_i e^{-\beta E_i}\partial E_i/\partial g^{-1}}{\sum_i e^{-\beta E_i}}, \end{aligned} \quad (2)$$

where E_i is the ith eigenenergy of the N-boson system and $\beta = (k_B T)^{-1}$. $C_N^c(g, T)$ can be exactly evaluated for $N = 2$ at any value of the interaction strength g and any temperature T, and in the Tonks-Girardeau limit $g \to \infty$ for any N and T.

Let us underline that analogously to the zero-temperature case, the contact can also be calculated from the average interaction energy that can be obtained by the free energy from the Hellmann-Feynman theorem $\langle H_{\rm int}\rangle = g\partial F/\partial g$ [42]. It follows [21] that

$$C_N^c(g,T) = \frac{gm^2}{\pi\hbar^4}\langle H_{\rm int}\rangle. \quad (3)$$

A. The two-boson system

For the two-boson system, the energy spectrum can be calculated analytically. In this case, $E_i = E_{cm,\ell} + E_{r,j}$, with $E_{cm,\ell}$ being the center-of-mass energy with quantum number ℓ and $E_{r,j} = \hbar\omega(1/2 + \nu_j)$ the relative energy, with quantum number j [$i = (\ell, j)$], that depends on the interaction strength via the implicit relation [12]

$$f(\nu) = \frac{\Gamma\left(-\frac{\nu}{2}\right)}{\Gamma\left(-\frac{\nu}{2}+\frac{1}{2}\right)} = -\sqrt{2}\frac{|a_{1D}|}{a_{ho}}, \quad (4)$$

where $\Gamma(x)$ is the gamma function [43]. $E_{cm,\ell}$, differently from the relative energy $E_{r,j}$, is completely independent of interatomic interactions as stated by the Kohn's theorem [44] and therefore does not contribute to the contact calculation. By applying Eq. (2), the two-boson contact then takes the form

$$\begin{aligned} C_2^c(g,T) &= \frac{\sqrt{8}z^2}{\pi a_{ho}^3}Z_r^{-1}\sum_j e^{-\beta\hbar\omega\nu_j}\frac{\partial\nu_j}{\partial z} \\ &= \frac{\sqrt{32}}{\pi a_{ho}^3}Z_r^{-1}\sum_j e^{-\beta\hbar\omega\nu_j}\frac{\Gamma\left(-\frac{\nu_j}{2}+\frac{1}{2}\right)}{\Gamma\left(-\frac{\nu_j}{2}\right)} \\ &\quad\times\left[\psi\left(-\frac{\nu_j}{2}+\frac{1}{2}\right) - \psi\left(-\frac{\nu_j}{2}\right)\right]^{-1}, \end{aligned} \quad (5)$$

where $Z_r = \sum_j e^{-\beta\hbar\omega\nu_j}$ is the canonical relative motion partition function and $\psi(x) = \Gamma'(x)/\Gamma(x)$ is the digamma function [43]. In the Tonks-Girardeau limit, $\nu_j = 2j - 1$ ($j \geqslant 1$) and both $\Gamma(-\frac{\nu_j}{2}+\frac{1}{2}) = \Gamma(-j+1)$ and $\psi(-\frac{\nu_j}{2}+\frac{1}{2}) = \psi(-j+1)$ diverge for $j \geqslant 1$. With some algebra, it can been shown that

$$C_2^c(\infty,T) = \frac{\sqrt{32}}{\pi^{3/2}a_{ho}^3}Z_r^{-1}\sum_j e^{-\beta\hbar\omega(2j-1)}\frac{(2j-1)!!}{2^j(j-1)!}. \quad (6)$$

Note that Eq. (6) gives the known limit $C_2^c(\infty, 0) = (2/\pi)^{3/2}a_{ho}^{-3}$ [37]. The canonical two-boson contact obtained by Eq. (5) is shown in Fig. 1. We have verified that the curve for $z = 1000$ is essentially indiscernible from the contact evaluated in the Tonks limit by means of Eq. (6).

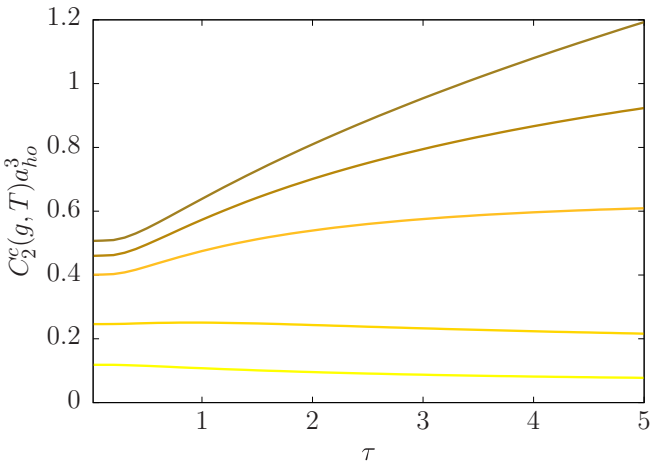

FIG. 1. Canonical Tan's contact $C_2^c(g,T)$ as a function of $\tau = T/T_F$ [Eq. (5)] for different values of the interaction strength $z = a_{ho}/(|a_{1D}|\sqrt{N})$. From bottom to top: $z = 0.5$, 1, 2.5, 5, and 1000. The curve for $z = 1000$ is indiscernible from the contact evaluated in the Tonks limit by means of Eq. (6).

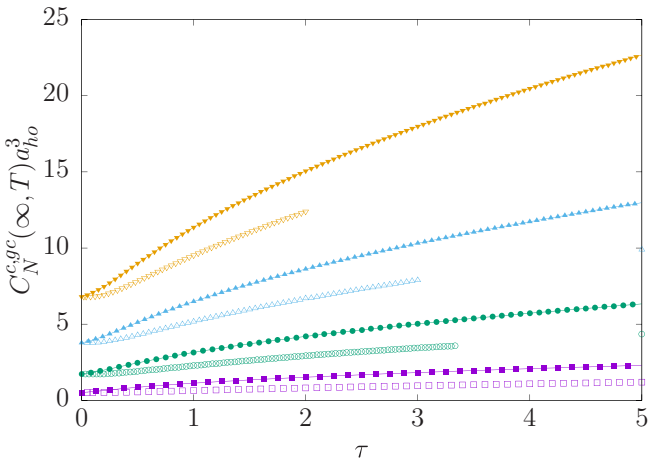

FIG. 2. Canonical contact (empty symbols) [Eq. (7)] and grand-canonical contact (full symbols) [46] as a function of τ for $N = 2$ (violet squares), $N = 3$ (green circles), $N = 4$ (light-blue up-triangles), and $N = 5$ (orange down-triangles) Tonks-Girardeau bosons. The grand-canonical case will be discussed in Sec. IV.

B. The Tonks-Girardeau limit

In the Tonks-Girardeau limit, where fermionization occurs, the interaction strength g is infinite, namely, the 1D scattering length a_{1D} is zero and therefore this length scale disappears by making the problem more universal. Thus the contact, in this regime, does not depend on the interactions and can be written as a function of the corresponding fermionic two-body density matrix $\rho_{2F}(x_1, x_2; x_1', x_2')$ [45]. More precisely, it can be shown that

$$C_N^c(\infty, T) = \frac{2}{\pi}\int_{-\infty}^{+\infty} dx F(x), \tag{7}$$

where we have defined

$$F(x) = \lim_{x',x''\to x} \frac{\rho_{2F}(x', x; x'', x)}{|x - x'||x - x''|}. \tag{8}$$

By explicitly expressing ρ_{2F} in the canonical ensemble, as a function of the single-particle orbitals $u_i(x)$, we get

$$\begin{aligned} F(x) = Z^{-1} \sum_{\substack{i_1=0,\infty, i_2=i_1+1,\infty \\ \dots i_{N_F}=i_{N_F-1}+1,\infty}} e^{-\beta\hbar\omega\sum_{j=1,N_F}(i_j+\frac{1}{2})} \\ \times \sum_{\langle j,k\rangle} \Big\{ \big[u_{i_j}(x)\partial_x u_{i_k}(x)\big]^2 \\ - 2u_{i_j}(x)\partial_x u_{i_k}(x) u_{i_k}(x)\partial_x u_{i_j}(x)\Big\}, \end{aligned} \tag{9}$$

with

$$Z = \sum_{\substack{i_1=0,\infty, i_2=i_1+1,\infty \\ \dots i_{N_F}=i_{N_F-1}+1,\infty}} e^{-\beta\hbar\omega\sum_{j=1,N_F}(i_j+\frac{1}{2})}. \tag{10}$$

The canonical contact $C_N^c(\infty, T)$, as obtained by Eqs. (7) and (9), is shown in Fig. 2 (empty symbols) for $N = 2$ to 5. The data are compared with grand-canonical ones [46] (full symbols) that will be discussed below (Sec. IV). Note that the computation of the contact is more demanding in the canonical case than in the grand-canonical one because of several sums in (9) that simplify in the grand-canonical case.

C. The finite interaction strength regime

In the finite interaction strength scenario for $N > 2$, we rely on quantum Monte Carlo simulations to obtain exact results. Starting from Eq. (1), we discretize the Hamiltonian using a finite-difference method and rewrite it using second quantization, ending with the following bosonic Hubbard Hamiltonian:

$$\begin{aligned} H = -t\sum_j (b_j^\dagger b_{j+1} - 2n_j + b_j^\dagger b_{j-1}) \\ + w\sum_j j^2 n_j + U\sum_j n_j(n_j - 1)/2. \end{aligned} \tag{11}$$

The discrete positions of the bosons are given by $x = j\Delta a_{ho}$, where Δ is a small dimensionless parameter. We typically used $\Delta = 0.1$ and checked on some simulations that the systematic errors induced by this discretization were smaller than the stochastic errors due to the Monte Carlo calculations. The operators $b_j^\dagger$ and b_j create or destroy bosons on site j. $n_j = b_j^\dagger b_j$ is the bosonic number operator on site j. The parameters are given by

$$t = \frac{\hbar\omega}{2\Delta^2},\ w = \frac{\hbar\omega\Delta^2}{2},\ U = \frac{g}{\Delta a_{ho}}. \tag{12}$$

The Hubbard model is simulated using the stochastic Green function algorithm [47,48] that allows the calculation of many physical quantities for finite systems at finite temperature. The algorithm works in both canonical and grand-canonical ensembles, although it is generally more efficient in the former case. Grand-canonical simulations require the sampling of a larger space containing different numbers of particles, which greatly increases the correlation time of the data, as the sampling of different N is not very efficient. Note that in the grand-canonical ensemble, it is then sometimes

difficult to pinpoint a precise value of $\langle N\rangle$ as it requires a fine tuning of the chemical potential μ.

We will concentrate on a small number of particles N, which gives a more thorough test of the scaling hypotheses that we will introduce as they should be valid for large N.

Using this algorithm, we calculate the average interaction energy $\langle H_{\rm int}\rangle$ that gives access to the contact [Eq. (3)]. We choose a system size large enough so density becomes zero at the edges of the system. As the temperature T increases, the simulations become increasingly difficult: the density distribution of the particles becomes wider, which means that the events where two particles are superposed and then contribute to the interaction energy become rare, giving a poor signal-to-noise ratio for the contact calculation. Increasing interactions also reduces the probability of double occupancies and, consequently, the precision of the calculation.

These difficulties are further enhanced by the fact that as N increases, we will maintain fixed rescaled temperature τ and interaction z to observe possible scaling behaviors. The temperature T and interaction g will then scale with the number of particles as N and $\sqrt{N}$, respectively. These combined effects strongly limit the temperatures, interactions, and number of particles for which we obtain reliable results. For canonical simulations, we were able to obtain results with a relative error better than two percent for rescaled interactions up to $z = 2.5$, rescaled temperatures up to $\tau = 5$, and numbers of particles up to $N = 5$. Grand-canonical results are more limited. For N up to 4, we are limited to $z = 1$ and $\tau = 0.2$ if we want a precision of few percents. For $N = 4$, $z = 1$, and $\tau = 2$, we have relative errors of the order of 20%, which hardly give meaningful information.

III. SCALING PROPERTIES

A. Zero-temperature scaling

In [37], we have shown that it is possible to express the contact for N bosons or N $SU(\kappa)$ fermions as a function of the contact for two bosons. Indeed, the reduced contact,

$$f_N(z,0) = \frac{C_N[g(z),0]}{C_N(\infty,0)}, \tag{13}$$

with $g(z) = 2\hbar^2\sqrt{N}z/(ma_{ho})$, verifies the relation [37]

$$f_N(z,0) \simeq f_2(z,0), \tag{14}$$

meaning that upon rescaling of the interaction strength, all the N dependence of the contact is in $C_N(\infty,0)$. Moreover, it has been shown from a fit on the numerical data [37] that

$$C_N[g(z),0] \sim N^{5/2} - \gamma N^{\eta}, \tag{15}$$

where $\gamma \simeq 1$ and $\eta = 3/4$ in the Tonks-Girardeau limit, and where they are slowly varying in the strongly interacting regime $z > 1$.

B. Large-temperature scaling

In the large-temperature limit, $T \gg T_F$, quantum correlations are negligible and the contact for N bosons in the canonical ensemble is simply given by the two-particle contact times the number of pairs,

$$C_N^c(g, T \gg T_F) = \frac{N(N-1)}{2} C_2^c(g, T \gg T_F). \tag{16}$$

In the strongly interacting limit, Eq. (16) takes the explicit form (see the Appendix)

$$\begin{aligned} C_N^c(z>1,\tau\gg 1) &= \frac{N(N-1)}{2}\frac{2g}{\pi^{3/2}\hbar\omega a_{ho}^4}\frac{1}{\sqrt{\alpha}} \\ &\quad\times\left[1-\sqrt{\frac{\pi}{\alpha}}e^{1/\alpha}\mathrm{Erfc}(1/\sqrt{\alpha})\right] \\ &= (N^{5/2}-N^{3/2})h_N(z>1,\tau\gg 1), \end{aligned} \tag{17}$$

with $\alpha = 4a_{ho}^2\hbar\omega/(\beta g^2) = \tau/z^2$ and

$$\begin{aligned} &h_N(z>1,\tau\gg 1) \\ &= \frac{2z}{\pi^{3/2}a_{ho}^3}\frac{1}{\sqrt{\alpha}}\left[1-\sqrt{\frac{\pi}{\alpha}}e^{1/\alpha}\mathrm{Erfc}(1/\sqrt{\alpha})\right]. \end{aligned} \tag{18}$$

In the Tonks-Girardeau limit,

$$\begin{aligned} C_N^c(\infty,\tau\gg 1) &= \frac{N(N-1)}{2}\frac{2}{\pi^{3/2}a_{ho}^3}\sqrt{\frac{k_BT}{\hbar\omega}} \\ &= (N^{5/2}-N^{3/2})h_N(\infty,\tau\gg 1), \end{aligned} \tag{19}$$

with

$$h_N(\infty,\tau\gg 1) = \frac{1}{\pi^{3/2}a_{ho}^3}\sqrt{\tau}. \tag{20}$$

Analogously to the zero-temperature case, we can define the function

$$f_N(z>1,\tau\gg 1) = \frac{C_N[g(z),T(\tau)]}{C_N[\infty,T(\tau)]}, \tag{21}$$

and we get that

$$f_N(z>1,\tau\gg 1) \simeq f_2(z>1,\tau\gg 1) \tag{22}$$

holds in the limit $T \gg T_F$, with $f_2(z>1,\tau\gg 1) = h_2(z>1,\tau\gg 1)/h_2(\infty,\tau\gg 1)$.

C. Any temperature scaling conjecture

We now propose the general scaling hypothesis that Eq. (22) holds for any temperature in the strong-interaction limit. This is equivalent to claim that upon rescaling of the interaction strength and of the temperature, all the N dependence of the contact is embedded in $C_N(\infty,T)$, for *any temperature*. This dependence is quite trivial at large temperature, as it is determined by the number of pairs, proportional to $N(N-1)$, and a $\sqrt{N}$ term that comes from the rescaling of the temperature with respect to the Fermi temperature. By lowering the temperature, the contact almost freezes at $T \simeq T_F$ and, because of quantum correlations, there is an enhancement of the dependence on N, from $N^{5/2}-N^{3/2}$ to $N^{5/2}-N^{3/4}$. This leads us to propose the following conjecture:

$$\begin{aligned} C_N^c(\infty,\tau) &= h_2(\infty,\tau)s(N) \\ &= h_2(\infty,\tau)(N^{5/2}-N^{3/4[1+\exp(-2/\tau)]}), \end{aligned} \tag{23}$$

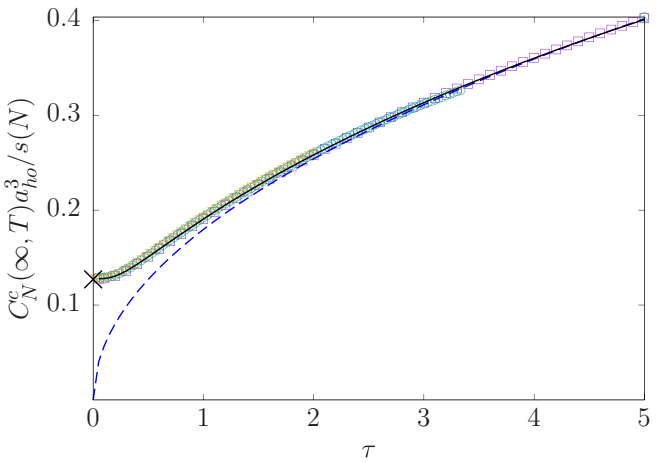

FIG. 3. Canonical contact in the Tonks-Girardeau limit $C_N(\infty, T)$, given by Eq. (7), as a function of τ, scaled by the factor $s(N) = N^{5/2} - N^{3/4[1+\exp(-2/\tau)]}$; see Eq. (23). Violet squares: $N = 2$; green circles: $N = 3$; light-blue up-triangles: $N = 4$; and orange down-triangles: $N = 5$. The blue dashed line corresponds to the high-temperature limit $h_2(\infty, \tau \gg 1)$ [Eq. (20)]. The black cross and the black line correspond to $h_2(\infty, 0) = (2/\pi)^{3/2} a_{ho}^{-3}(2^{5/2} - 2^{3/4})^{-1}$ and $h_2(\infty, \tau)$ [Eq. (24)], respectively.

where

$$h_2(\infty, \tau) = C_2[\infty, T(\tau)]/s(2) \tag{24}$$

can de derived by Eq. (6). In Fig. 3, we plot $C_N^c(\infty, T)$ [Eq. (7)], divided by $s(N)$, as a function of τ, for cases from $N = 2$ to $N = 5$, as well as $h_2(\infty, \tau)$, its high-temperature limit $h_2(\infty, \tau \gg 1)$, and its value at zero temperature, $h_2(\infty, 0)$. All the data collapse on the same curve $h_2(\infty, \tau)$ (continuous black curve), showing that the conjecture (23) works extremely well. We test now the reliability of the generalized scaling hypothesis

$$f_N(z > 1, \tau) \simeq f_2(z > 1, \tau) \tag{25}$$

approaching the strongly interacting regime. In Figs. 4 and 5, we plot the canonical contact, obtained from quantum Monte Carlo simulations, for the cases $z = 1$ and 2.5, respectively.

For both Figs. 4 and 5, in panels (a) the data have been rescaled by $N^{5/2} - N^{3/4}$, in panels (b) by $N^{5/2} - N^{3/2}$, and in panels (c) by $s(N)$. The "zero-temperature" scaling factor $N^{5/2} - N^{3/4}$, as obtained in [37] for the Tonks-Girardeau limit, makes, at small temperatures, the curves approach at $z = 1$ and collapse at $z = 2.5$. The "pair scaling" term $N^{5/2} - N^{3/2}$ works well in the large-temperature regime $\tau > 1$, while the interpolating function $s(N)$ [Eq. (23)] allows the collapse of the data in the whole temperature range, with an incertitude of 5% for the case $z = 1$ [Fig. 4(c)] and of 1% for the case $z = 2.5$ [Fig. 5(c)]. The validity of the scaling hypothesis (25) is verified in Figs. 4(d) and 5(d). Note that as mentioned earlier, precise QMC results are limited to a small number of particles and intermediate values of τ and z. The limitation on the number of particles is not crucial as, for large number of particles, $\lim_{N\to\infty} s(N)/N^{5/2} = 1$, and we recover the known thermodynamics limit. Concentrating on a small number of particles $N \leqslant 5$ then provides a more stringent verification of the reliability of the scaling hypothesis (25).

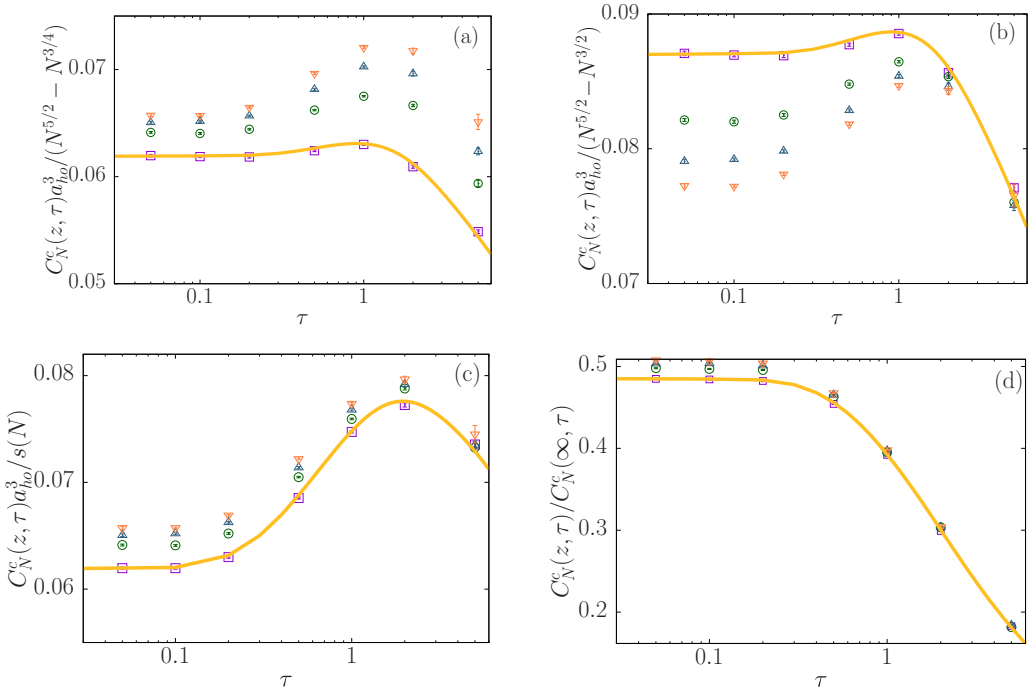

FIG. 4. $C_N^c(z, \tau)a_{ho}^3$ as a function of τ, for the case $z = 1$, rescaled by (a) $N^{5/2} - N^{3/4}$, (b) $N^{5/2} - N^{3/2}$, and (c) $s(N)$. (d) $f_N(z = 1, \tau)$ as a function of τ. The points (violet squares: $N = 2$; green circles: $N = 3$; light-blue up-triangles: $N = 4$; and orange down-triangles: $N = 5$) correspond to the QMC data. The continuous yellow line corresponds to the two-boson contact obtained by Eq. (5). Nonvisible QMC error bars are smaller than the symbol size.

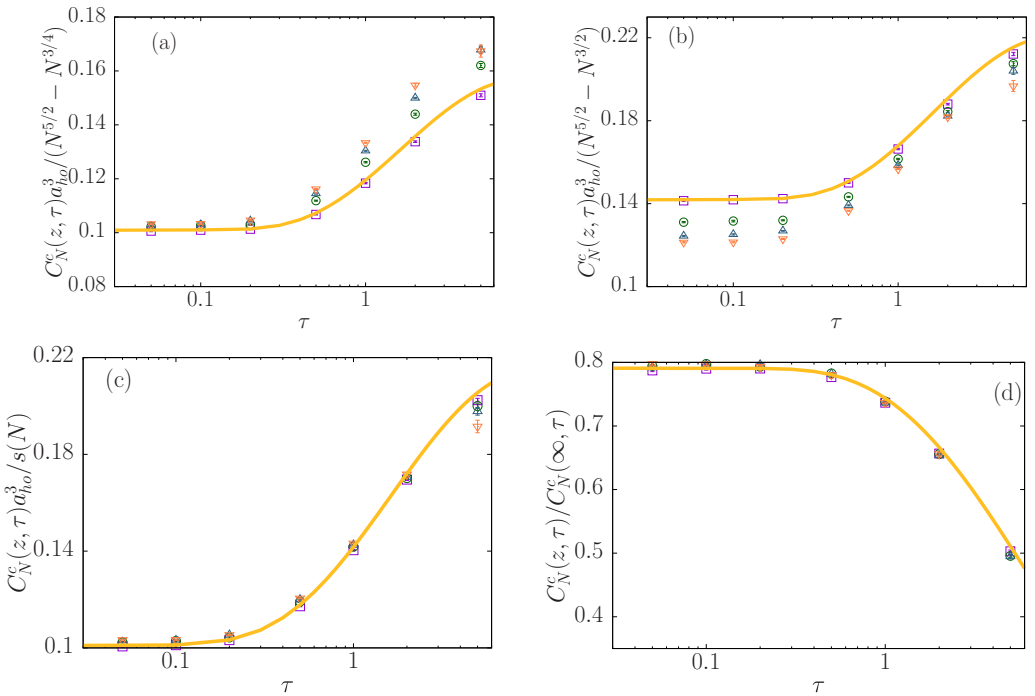

FIG. 5. $C_N^c(z,\tau)a_{ho}^3$ as a function of τ, for the case $z = 2.5$, rescaled by (a) $N^{5/2} - N^{3/4}$, (b) $N^{5/2} - N^{3/2}$, and (c) $s(N)$. (d) $f_N(z = 2.5, \tau)$ as a function of τ. The points (violet squares: $N = 2$; green circles: $N = 3$; light-blue up-triangles: $N = 4$; and orange down-triangles: $N = 5$) correspond to the QMC data. The continuous yellow line corresponds to the two-boson contact obtained by Eq. (5). Nonvisible QMC error bars are smaller than the symbol size.

IV. COMPARISON WITH THE GRAND-CANONICAL TAN'S CONTACT

In the zero-temperature limit, the grand-canonical and canonical contacts coincide, and thus, in the strongly interacting regime, both scale as $\sim(N^{5/2} - N^{3/4})$.

But, as soon as the temperature increases, the grand-canonical contact for an average number $\langle N\rangle$ of particles departs from the canonical one for N particles. Indeed, with larger number contributions, the grand-canonical contact increases more rapidly than the canonical one that is almost constant for $0 \leqslant \tau \leqslant 0.5$ (see Fig. 2 for the Tonks-Girardeau limit case).

In the large-temperature limit, in the grand-canonical ensemble, the term $N(N-1)$, proportional to the number of pairs in the canonical ensemble, has to be replaced by its average value,

$$\langle N(N-1)\rangle = \langle N^2\rangle - \langle N\rangle = \langle N\rangle^2. \tag{26}$$

This follows from the fact that at large T, $\langle \Delta N^2\rangle \simeq \langle N\rangle$. By defining $T_F = \langle N\rangle\hbar\omega/k_B$, we find

$$C_N^{gc}(g, T \gg T_F) = \frac{\langle N\rangle^2}{2} C_2^c = \langle N\rangle^{5/2} h_2(z > 1, \tau \gg 1), \tag{27}$$

in agreement with the virial calculation [16]. Thus, in the large-temperature limit, $C_N^{gc}(g, T \gg T_F)/\langle N\rangle^{5/2}$ and $C_N^c(g, T \gg T_F)/(N^{5/2} - N^{3/2})$ collapse on the same curve, $h_2(z, \tau \gg 1) = \sqrt{\tau}/(\pi^{3/2} a_{ho}^3)$. This is shown in Fig. 6 for the Tonks-Girardeau limit, where we have compared the canonical contact [Eq. (7)] and the grand-canonical one as obtained from Eqs. (8) and (9) in [46]. Note that the convergence is faster for the grand-canonical contact. The consequence of the fact that the canonical and the grand-canonical contacts are proportional to one another, at large temperature $\tau \gg 1$, is that both have a maximum at $\tau = 1.48z^2$ in the strong-interacting limit [16]. The situation is different in the weak-interaction regime, where the grand-canonical contact exhibits

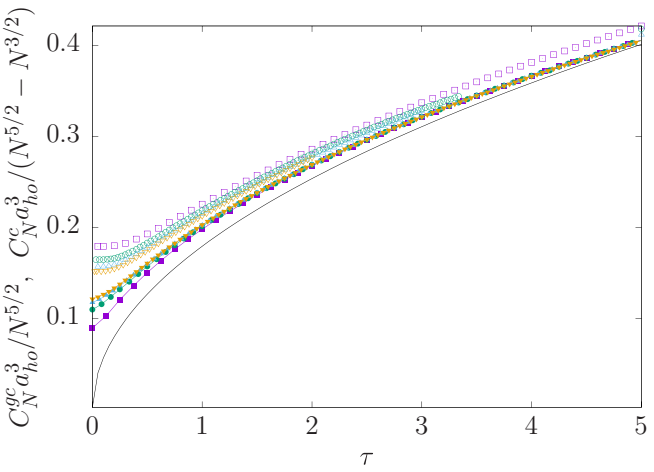

FIG. 6. Canonical (empty symbols) and grand-canonical contact (full symbols) as a function of τ for $N = 2$ (violet squares), $N = 3$ (green circles), $N = 4$ (light-blue up-triangles), and $N = 5$ (orange down-triangles) Tonks-Girardeau bosons. The canonical contact [Eq. (7)] is rescaled by a factor $N^{5/2} - N^{3/2}$, while the grand-canonical one (Eqs. (8) and (9) in [46]) is rescaled by $N^{5/2}$. The black continuous curve corresponds to $\sqrt{\tau}/\pi^{3/2}$ [Eq. (20)].

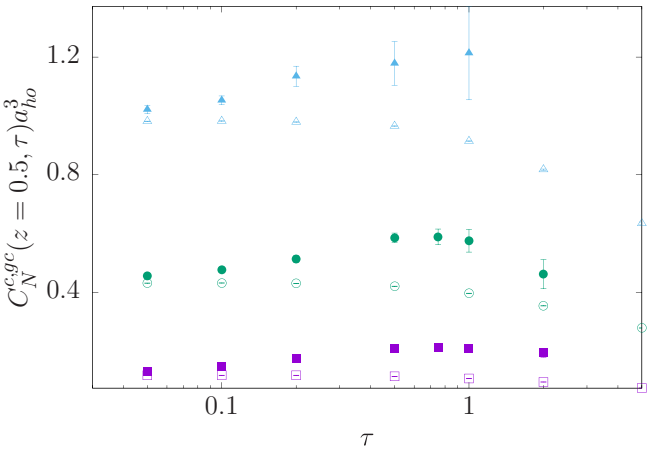

FIG. 7. Canonical (empty symbols) and grand-canonical contact (full symbols) as a function of τ for $N = 2$ (violet squares), $N = 3$ (green circles), and $N = 4$ (light-blue up-triangles) bosons. All points correspond to QMC data evaluated in the weakly interacting regime $z = 0.5$. QMC error bars for the canonical data are smaller than the symbol size.

a maximum at lower temperatures. This maximum, which has been explained as the mark of the crossover between a quasicondensate and an ideal Bose gas [16], is not present in the canonical case. This has been studied by means of QMC simulations and shown in Fig. 7.

In the canonical ensemble and at low interactions, the contact decreases with increasing temperature because as particles occupy individual excited states, the cloud of particles spreads and the interaction energy is lowered. This happens when the temperature is large enough to overcome the $\hbar\omega$ gap between the ground and excited states, which explains why there is almost no variation at low temperature.

In the grand-canonical ensemble, the same effect will of course take place and yields to the same decrease of the contact at high temperature. However, at low temperature, another phenomena occurs: the probability to have a number of particles that is larger than $\langle N\rangle$ increases with temperature. This gives larger contributions to the interaction energy and explains the initial increase of the contact at low temperatures.

As Eq. (22) holds even in the grand-canonical ensemble, one may wonder if the generalized scaling hypothesis (25) is still valid in this ensemble. In Fig. 8, we plot the quantity $C_N^{gc}(z,\tau)/C_N^{gc}(\infty,\tau)$ for the case $z = 1$ and $N = 2$, 3, and 4 and $\tau \leqslant 2$, $C_N^{gc}(z,\tau)$ having been calculated by means of QMC simulations and $C_N^{gc}(\infty,\tau)$ by means of Eqs. (8) and (9) in [46]. We observe that for small and intermediate temperatures, in the intermediate-interactions regime, the curves remain different instead of the collapse observed in the canonical case [see Fig. 4(d)]. Our scaling hypothesis then fails in this case of intermediate interactions, as the grand-canonical Tonks-Girardeau contact does not embed the full $\langle N\rangle$ dependency for these intermediate interactions. We were not able to test this scaling hypothesis in the grand-canonical ensemble at larger interactions as QMC simulations become increasingly difficult.

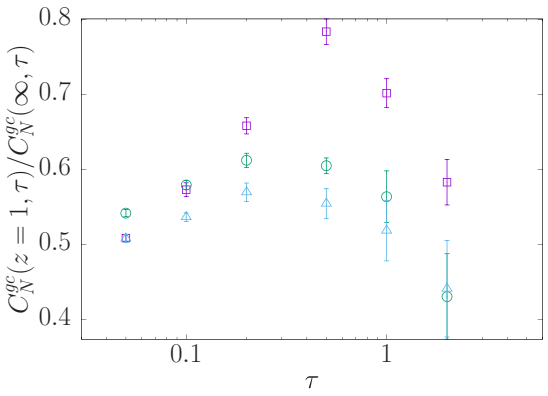

FIG. 8. $C_N^{gc}(z = 1,\tau)/C_N^{gc}(\infty,\tau)$ as a function of τ. The points (violet squares: $N = 2$; green circles: $N = 3$; light-blue up-triangles: $N = 4$) correspond to the QMC data.

V. CONCLUSION

In this paper, we have shown that the canonical contact for N harmonically trapped, Lieb-Liniger bosons, at any temperature, in the repulsive strongly interacting regime, can be written as a function of the two-boson contact and the contact for N Tonks-Girardeau bosons. The first can be easily calculated and we provide an analytical formula for the second for any number of bosons and temperature. This enlightens the dependence of the contact on the number of pairs at large temperature and the effects of correlations at low temperature. Moreover, it supplies a scaling function, in the canonical ensemble, for any number of particles $N \geqslant 2$ and any temperature in the strong-interacting regime. We have proven our theory for a small number of bosons ($2 \leqslant N \leqslant 5$), where corrections with respect to the known thermodynamic limit are more important. We have been informed that these results may also hold true for a 1D homogeneous Bose gas. This can be deduced from the results recently presented in [49]. In this paper, the authors show that in the strongly interacting limit, $C_N^c = 4mNP_H/\hbar^2$. The force P_H is expressed as $P_H = n^3 f_H(z_H,\tau_H)$, where $z_H = (na_{1D})^{-1}$ is the rescaled interaction strength for the homogeneous system of linear density n, $\tau_H = T/T_{F,H}$ is the rescaled temperature ($T_{F,H}$ being the Fermi temperature for the homogeneous system), and f_H is a universal function of z_H and τ_H. From this, it can be deduced that $C_N^c(z_H > 1,\tau_H)/C_N^c(\infty,\tau_H)$ is also a universal function, which is equivalent for a homogeneous system of the scaling relations found in the trapped case.

Finally, we discuss the difference between the canonical and grand-canonical contacts. At large temperature, these quantities are both proportional to the two-boson contact, and the proportionality factor depends on the number of pairs in the canonical ensemble and the average number of pairs in the grand-canonical one. The main difference between the grand-canonical and canonical cases is that at small and intermediate temperatures, the grand-canonical contact for $\langle N\rangle$ bosons cannot be written as a function of the $\langle 2\rangle$-boson contact and the contact for $\langle N\rangle$ Tonks-Girardeau bosons, as far as we can test it with the QMC simulations in the intermediate-interaction regime. Namely, at variance from the canonical case, the grand-canonical contact for $\langle N\rangle$ Tonks-Girardeau

bosons seems not to embed the dependence for the average number of particles $\langle N \rangle$. Indeed, our scaling hypothesis fails as far as we can test it with the QMC simulations in the intermediate-interaction regime.

Our work can be relevant for experiments with a small number of particles [50,51]. From a conceptual point of view, it is an important step forward in understanding the effects of correlations and interactions in finite-temperature, harmonically trapped, one-dimensional bosons, as well as in grasping the role of the particle-number fluctuations. The extension to the case of multicomponent systems is not straightforward and will be the subject of a further study.

ACKNOWLEDGMENTS

We thank an anonymous referee for many useful suggestions and, in particular, for making us aware that our results hold even in the 1D untrapped Bose gas. P.V. thanks A. Minguzzi for useful discussions. The work of F.T.S. was financed in part by the Coordenação de Aperfeiçoamento de Pessoal de Nível Superior - Brasil (CAPES) - Finance Code 001.

APPENDIX : TWO-BODY CONTACT IN THE STRONG INTERACTION AND LARGE-TEMPERATURE LIMIT

We start with Eq. (5),

$$C_2^c = -\frac{m^2\omega}{\pi\hbar^3} Z_r^{-1} \sum_n e^{-\beta\hbar\omega\nu_n} \frac{\partial \nu_n}{\partial g^{-1}}. \tag{A1}$$

It can be shown [16] that in the strongly interacting limit $z > 1$, the solutions of Eq. (4) are given by

$$\nu_n \simeq \frac{2}{\pi}\mathrm{acot}(2\sqrt{2n+1}g^{-1}\hbar\omega a_{ho}) + 2n, \tag{A2}$$

with $n \geqslant 0$. This approximation (A2) becomes more precise at large values of n. Thus, (A1) reads

$$C_2^c = \frac{4Z_r^{-1}}{\pi^2 a_{ho}^3} \sum_n \frac{e^{-\beta\hbar\omega\nu_n}\sqrt{2n+1}}{1+4(2n+1)(\hbar\omega a_{ho} g^{-1})^2}. \tag{A3}$$

By replacing in the exponential ν_n with its value in the Tonks-Girardeau limit, $\nu_n = 2n+1$, and exploiting that

$$\int_0^\infty \frac{\sqrt{x}}{1+xb^2} e^{-\beta\hbar\omega x} dx = \frac{1}{(\beta\hbar\omega)^{3/2}} \frac{\sqrt{\pi}}{\alpha}\left[1 - \sqrt{\frac{\pi}{\alpha}} e^{1/\alpha}\mathrm{Erfc}(1/\sqrt{\alpha})\right], \tag{A4}$$

with $\alpha = b^2/(\hbar\omega\beta) = 4a_{ho}^2\hbar\omega/(\beta g^2)$, we have that

$$C_2^c = \frac{2g}{\pi^{3/2}\hbar\omega a_{ho}^4} \frac{1}{\sqrt{\alpha}}\left[1 - \sqrt{\frac{\pi}{\alpha}} e^{1/\alpha}\mathrm{Erfc}(1/\sqrt{\alpha})\right]. \tag{A5}$$

Note that Eq. (A5) is valid only in the large-temperature limit where replacing the sum with an integral is a valid approximation. Hence, in the Tonks-Girardeau limit, the contact reduces to

$$\lim_{g\to\infty} C_2^c = \frac{2}{\pi^{3/2} a_{ho}^3}\sqrt{\frac{k_B T}{\hbar\omega}}. \tag{A6}$$

[1] E. Lieb and W. Liniger, Phys. Rev. **130**, 1605 (1963).
[2] J. B. McGuire, J. Math. Phys. (NY) **5**, 622 (1964).
[3] C. N. Yang and C. P. Yang, J. Math. Phys. **10**, 1115 (1969).
[4] E. Lieb, Phys. Rev. **130**, 1616 (1963).
[5] C. N. Yang, Phys. Rev. Lett. **19**, 1312 (1967).
[6] M. Gaudin, Phys. Lett. **24**, 55 (1967).
[7] B. Sutherland, Phys. Rev. Lett. **20**, 98 (1968).
[8] C. K. Lai and C. N. Yang, Phys. Rev. A **3**, 393 (1971).
[9] J. B. McGuire, J. Math. Phys. (NY) **6**, 432 (1965).
[10] A. Luther and V. J. Emery, Phys. Rev. Lett. **33**, 589 (1974).
[11] J. N. Fuchs, A. Recati, and W. Zwerger, Phys. Rev. Lett. **93**, 090408 (2004).
[12] T. Busch, B.-G. Englert, K. Rzążewski, and M. Wilkens, Found. Phys. **28**, 549 (1998).
[13] A. Aharony, O. Entin-Wohlman, and Y. Imry, Phys. Rev. B **61**, 5452 (2000).
[14] J. Abad and J. G. Esteve, Few-Body Syst. **37**, 107 (2005).
[15] M. Olshanii and V. Dunjko, Phys. Rev. Lett. **91**, 090401 (2003).
[16] H. Yao, D. Clément, A. Minguzzi, P. Vignolo, and L. Sanchez-Palencia, Phys. Rev. Lett. **121**, 220402 (2018).
[17] T. Giamarchi, *Quantum Physics in One Dimension* (Clarendon Press, Oxford, 2003).
[18] E. Gross, Il Nuovo Cimento **20**, 454 (1961).
[19] L. Pitaevskii, Sov. Phys. JEPT **13**, 451 (1961).
[20] S. Tan, Ann. Phys. (NY) **323**, 2971 (2008).
[21] S. Tan, Ann. Phys. (NY) **323**, 2987 (2008).
[22] S. Tan, Ann. Phys. (NY) **323**, 2952 (2008).
[23] J. T. Stewart, J. P. Gaebler, T. E. Drake, and D. S. Jin, Phys. Rev. Lett. **104**, 235301 (2010).
[24] Y. Sagi, T. E. Drake, R. Paudel, and D. S. Jin, Phys. Rev. Lett. **109**, 220402 (2012).
[25] R. Chang, Q. Bouton, H. Cayla, C. Qu, A. Aspect, C. I. Westbrook, and D. Clément, Phys. Rev. Lett. **117**, 235303 (2016).
[26] R. J. Wild, P. Makotyn, J. M. Pino, E. A. Cornell, and D. S. Jin, Phys. Rev. Lett. **108**, 145305 (2012).
[27] Z. Yan, P. B. Patel, B. Mukherjee, R. J. Fletcher, J. Struck, and M. W. Zwierlein, Phys. Rev. Lett. **122**, 093401 (2019).
[28] S. Hoinka, M. Lingham, K. Fenech, H. Hu, C. J. Vale, J. E. Drut, and S. Gandolfi, Phys. Rev. Lett. **110**, 055305 (2013).
[29] S. Laurent, M. Pierce, M. Delehaye, T. Yefsah, F. Chevy, and C. Salomon, Phys. Rev. Lett. **118**, 103403 (2017).
[30] J. Decamp, J. Jünemann, M. Albert, M. Rizzi, A. Minguzzi, and P. Vignolo, Phys. Rev. A **94**, 053614 (2016).
[31] J. Decamp, J. Jünemann, M. Albert, M. Rizzi, A. Minguzzi, and P. Vignolo, New J. Phys. **19**, 125001 (2017).
[32] A. Minguzzi, P. Vignolo, and M. Tosi, Phys. Lett. A **294**, 222 (2002).
[33] T. Grining, M. Tomza, M. Lesiuk, M. Przybytek, M. Musial, R. Moszynski, M. Lewenstein, and P. Massignan, Phys. Rev. A **92**, 061601(R) (2015).

[34] N. Matveeva and G. Astrakharchik, New J. Phys. **18**, 065009 (2016).
[35] O. I. Pâţu and A. Klümper, Phys. Rev. A **93**, 033616 (2016).
[36] W. Xu and M. Rigol, Phys. Rev. A **92**, 063623 (2015).
[37] M. Rizzi, C. Miniatura, A. Minguzzi, and P. Vignolo, Phys. Rev. A **98**, 043607 (2018).
[38] H. Moritz, T. Stöferle, M. Köhl, and T. Esslinger, Phys. Rev. Lett. **91**, 250402 (2003).
[39] G. Pagano, M. Mancini, G. Cappellini, P. Lombardi, F. Schäfer, H. Hu, X.-J. Liu, J. Catani, C. Sias, M. Inguscio, and L. Fallani, Nat. Phys. **10**, 198 (2014).
[40] F. Salces-Carcoba, C. J. Billington, A. Putra, Y. Yue, S. Sugawa, and I. B. Spielman, New J. Phys. **20**, 113032 (2018).
[41] M. Olshanii, Phys. Rev. Lett. **81**, 938 (1998).
[42] M. Valiente, EPL **98**, 10010 (2012).
[43] I. Gradshteyn and I. Ryzhik, *Table of Integrals, Series, and Products* (Elsevier, Amsterdam, 1996).
[44] L. Pitaevskii and S. Stringari, *Bose-Einstein Condensation and Superfluidity* (Oxford University Press, Oxford, 2016).
[45] B. Y. Fang, P. Vignolo, C. Miniatura, and A. Minguzzi, Phys. Rev. A **79**, 023623 (2009).
[46] P. Vignolo and A. Minguzzi, Phys. Rev. Lett. **110**, 020403 (2013).
[47] V. G. Rousseau, Phys. Rev. E **77**, 056705 (2008).
[48] V. G. Rousseau, Phys. Rev. E **78**, 056707 (2008).
[49] G. D. Rosi, P. Massignan, M. Lewenstein, and G. E. Astrakharchik, Phys. Rev. Research **1**, 033083 (2019).
[50] G. Zürn, F. Serwane, T. Lompe, A. N. Wenz, M. G. Ries, J. E. Bohn, and S. Jochim, Phys. Rev. Lett. **108**, 075303 (2012).
[51] A. N. Wenz, G. Zürn, S. Murmann, I. Brouzos, T. Lompe, and S. Jochim, Science **342**, 457 (2013).